

RERTR 2011 — 33<sup>rd</sup> INTERNATIONAL MEETING ON  
REDUCED ENRICHMENT FOR RESEARCH AND TEST REACTORS

October 23-27, 2011  
Marriott Santiago Hotel  
Santiago, Chile

**INTERACTIONS BETWEEN UMo/Al FUEL AND DIFFUSION BARRIERS Nb  
AND TiN UNDER HEAVY ION IRRADIATION**

H.-Y. Chiang, R. Jungwirth, T. Zweifel, W. Schmid and W. Petry  
Physik-Department E13,  
and  
Forschungsneutronenquelle Heinz Maier-Leibnitz (FRM II),  
Technische Universität München  
Lichtenbergstr. 1, 85747 Garching (Germany)

and

F. Kraus  
AG Fluorchemie  
Fakultät für Chemie, Technische Universität München,  
Lichtenbergstr. 4, 85747 Garching (Germany)

**ABSTRACT**

The stability of the interaction layer between U-Mo fuel and Al matrix can be improved by adding alloying elements in the aluminum matrix or in the U-Mo alloy [1]. It is also observed that the growth of the interaction layer during in-situ irradiation can be suppressed by adding a diffusion barrier element. To understand the interactions among UMo, diffusion barriers and Al matrix, a sandwich structure has been fabricated. First a diffusion barrier of niobium or titanium nitride has been sputtered on an Al substrate, and then covered by an UMo top layer. With the purpose to simulate typical in-pile irradiation conditions these two sandwich structures have been subjected to iodine ion irradiation with the purpose to simulate typical in-pile irradiation conditions: 80 MeV  $I^{6+}$  ions and a fluence of  $1 \times 10^{17}/\text{cm}^2$ . Ions impinge the sample from the UMo side. Post irradiation examinations prove the complete suppression of the diffusion induced interaction layer (IDL). However, atomic mixing in both sandwich structures is observed.

**1. Introduction**

Uranium-molybdenum/aluminum dispersion fuel is developed for high-performance research reactors such as FRM II to replace highly-enriched fuel currently used [2]. However, it is observed that during in-pile tests, an irradiation induced interdiffusion layer (IDL) forms at the interface of U-Mo and Al matrix which influences the irradiation performance by increasing the dimensions and decreasing the thermal conductivity of the fuel [3-6]. Furthermore, large fission gas bubbles have been found at the interface between the U-Mo/Al interaction layer and the Al matrix [7-9]. These are responsible for anomalous swelling of the fuel plates. Therefore, the research on the behavior of the interaction layer to

mitigate the diffusion reaction is highlighted. The compositions of the intermetallic phases in the interaction layer range from (U,Mo)Al<sub>5</sub> to (U,Mo)Al<sub>7</sub> [10]. It is considered that the phases with high Al content are less stable during the irradiation. To minimize the amount of high-Al-content phases, modifications of U-Mo/Al by adding alloying elements in the Al matrix [11-14] or U-Mo alloy [15-18] have been proposed. Here we follow an alternative approach, i.e. direct coating of the UMo with a diffusion barrier [19-22]. The selection of the coating materials is guided by thermodynamics. The selected materials are sputtered between the U-Mo and Al layer and subjected to I<sup>6+</sup> irradiation at 80 MeV to observe the behavior of the interaction layer. This heavy ion irradiation simulates out-of-pile fission damages caused by fission fragments. This out-of-pile test is fast and it is easy to perform to post irradiation investigations.

## 2. Material Selections

Two materials, niobium and titanium nitride are coated between U-Mo and Aluminum layer. Nb has been used as a diffusion barrier in U-Mo/ Al fuel [20] and it reduces the swelling after irradiation. From the phase diagrams, it is seen that Nb has little solubility with U ( $T \leq 500$  °C) and Al ( $T \leq 660$  °C) [23]. Nb forms no specific compound with U but can form rather stable compounds with Al. The interaction between Nb and Al is predicted under the considerations from the interplanar spacing and heat of mixing. Al-Nb is a chemically miscible system with a negative heat of mixing of  $-18$  J/mol [24]. The strength of Al-Nb interatomic bond at interface is stronger than that of Al-Al and Nb-Nb bonds. N. Li et al. [25] indicate that under He ion irradiation Nb<sub>3</sub>Al can be generated as a consequence of radiation induced mixing in Al/Nb multilayers. In a comparison with Al, Nb<sub>3</sub>Al is densely packed with stronger interatomic bonds. One can expect that with such a dense intermetallic layer Nb<sub>3</sub>Al can prevent further intermixing of Nb and Al during irradiation.

Titanium nitride is commonly used as a protective coating and known as a barrier material. As a ceramic material, TiN is chemically stable. A.L. Izhotov et al. have shown that interstitial nitrides such as ZrN, as a coating on U-Mo powders, barriers Al from U completely during in-pile test [26]. For SELENIUM project UMo powder has been coated with ZrN. Recent characterization of fuel plate made of this coated powder indicates that during the process of plate fabrication, the ZrN coating may crack and an interaction will grow from these cracks [27]. This undesirable effect is due to the brittleness of ZrN. As a member of interstitial nitrides, TiN has better mechanical property than ZrN such as less modulus of elasticity  $\lambda = \text{stress/strain}$  (ZrN: 397 GPa and TiN: 251 GPa). Based on this advantage, TiN is believed to be a potential candidate as a diffusion barrier.

One should also consider the thermal neutron cross-sections of these materials. The total neutron cross-section the most common diffusion barrier ranks from highest to the lowest as N (12.5 b), Ti (10.8 b), Nb (7.8 b), Zr (6.8 b), and Si (2.4 b) at  $E = 0.025$  eV [28]. These neutron cross-sections are within the acceptable regimes for use in fuel materials.

The sandwich structures are fabricated by DC magnetron sputtering [31] and reactive sputtering [32]. The U-Mo alloy layers and Nb layers are coated by DC magnetron sputtering in our own laboratory whereas the TiN layers are fabricated by reactive sputtering at the Fakultät für Elektro- und Informationstechnik of TU Munich. A U8wt%Mo target has been used. Note: after the reactive sputtering of TiN, the sample is bent slightly with the curvature in the middle i.e. internal stresses are built during the fabrication. These layers are sputtered on Al substrates with a thickness of 0.5 mm. The details of samples are listed in Table 1.

	<b>barrier thickness (μm)</b>	<b>U-Mo thickness (μm)</b>
<b>UMo/Al</b>	0	4.5
<b>UMo/Nb/Al 1</b>	1.5	3.3
<b>UMo/Nb/Al 2</b>	1.5	2.3
<b>UMo/TiN/Al 1</b>	0.45	3.3
<b>UMo/TiN/Al 2</b>	0.23	3.3

Tab. 1. The information of samples: barrier thicknesses and the thicknesses of U-Mo layers during irradiation.

### 3. Heavy Ion Irradiation

When  $^{235}\text{U}$  undergoes fission, neutrons, fission fragments, beta particles, neutrinos and gamma irradiation come along with the process [29]. Among all these products, neutrons and fission fragments are considered to account for the radiation damages and phase changes of fuel materials. These high energy neutrons and fission fragments make collisions with materials inside the fuel core and induce damages. An irradiation induced diffusion layer grows at the interface between the U-Mo alloy and the Al matrix. Out-of-pile tests like ion irradiation are often applied to understand the mechanisms of radiation induced damages in materials. To simulate the growth of interaction layers, heavy ion irradiation can be an ideal method. The selection of ion species and energy are based on the principle of simulating the thermal fission process. Thermal fission shows that the mass distribution of fission fragments has two peaks at  $A = 95$  amu and  $A = 137$  amu. Fission fragments have 80% of the fission energy after the reaction and it means the lighter fragment has 98 MeV and the heavier one has 68 MeV as kinetic energy [30]. Therefore iodine ion with 80 MeV is considered as one of the most suitable ions for simulating the damages caused by fission fragments [1]. Iodine ion irradiation is carried out at the Maier-Leibnitz-Laboratorium, Garching (Germany). With the 14 MW Tandem accelerator, iodine ions with six-fold positive charge and 80 MeV energy are generated. The irradiation is carried out under high vacuum conditions ( $P \leq 10^{-5}$  mbar). Target temperatures are determined by ion collisions and are documented by thermal sensor (PT100). With an average current of 600 nA, the target temperature is around 200 °C during the irradiation. The samples are subjected to iodine ion irradiation: 80 MeV  $\text{I}^{6+}$  ions and a fluence of  $1 \times 10^{17}/\text{cm}^2$ . This total fluence corresponds to 3.5 - 4.7 % of the peak burn up of the FRM II fuel element at EOL [33].

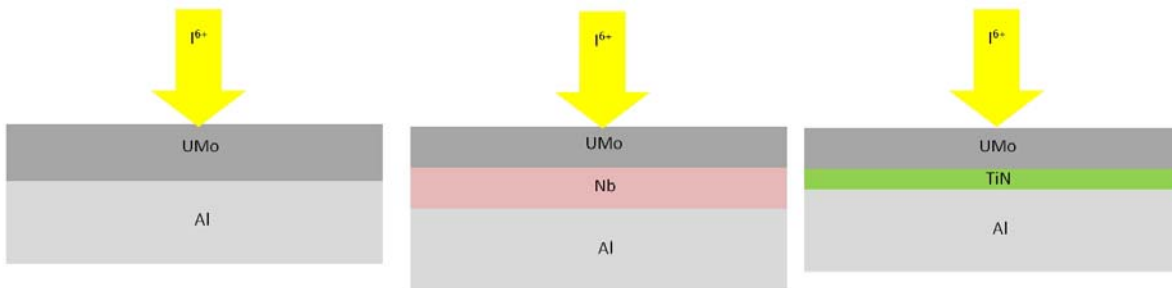


Fig. 1. Sketches of different sandwich structures.

### 4. Thermodynamic considerations

Ion irradiation is considered as a term of energy transfer to nuclei and electrons of the target. This is a non-equilibrium state. Even though thermodynamics is constructed under the condition of equilibrium, one can still use it to make cautious predictions on the irradiation products. So thermochemical effects play an important role in biasing the random walk process of mixing during irradiation [34]. Based on thermodynamics, reactions can be predicted by the value of enthalpy. The enthalpy of formation ( $\Delta H^{\text{for}}$ ) gives a prediction of reactions between materials.

The enthalpies of formation for Nb in binary alloy system are shown in Table 2. Nb exhibits a tendency to form compounds with Al and Mo. The possible Nb-Al compounds are  $\text{NbAl}_3$ ,  $\text{Nb}_2\text{Al}$ , and  $\text{Nb}_3\text{Al}$ . The possible Nb-Mo compound is  $\text{NbMo}$ . From a thermodynamic point of view Nb-U interaction does not exist. There is no possible compound and the positive values of limiting partial enthalpies of solution,  $\Delta H^{\circ}_{\{\text{Nb}\}}$  (+ 15 kJ/mole of atoms),  $\Delta H^{\circ}_{\{\text{U}\}}$  (+ 4 kJ/mole of atoms), and  $\Delta H^{\text{mix}}_{\{\text{NbU}\}}$  (+ 17 kJ/mole of atoms) [24] keep Nb away from U. One can expect there will be no interaction between U and Al in UMo/Nb/Al structures.

The enthalpies of formation of Ti in the binary alloy systems are listed in Table 3. Ti has a tendency to form compounds with Al and Mo. The possible Ti-Al compounds are  $\text{TiAl}_3$ ,  $\text{TiAl}$ ,  $\text{Ti}_3\text{Al}$ , and  $\text{Ti}_{88}\text{Al}_{12}$ . The possible Ti-Mo compound is  $\text{Ti}_{50}\text{Mo}_{50}$ . U has no tendency to form chemical compound with Ti but solid solution with Ti. Though there are possibilities of the formation of Ti-Al compounds, yet TiN is

considered chemical more stable than Ti and immiscible [35]. It is deduced that no U-Al interaction will occur in UMo/TiN/Al.

	NbX <sub>5</sub>	NbX <sub>3</sub>	NbX <sub>2</sub>	Nb <sub>3</sub> X <sub>5</sub>	Nb <sub>2</sub> X <sub>3</sub>	NbX	Nb <sub>5</sub> X <sub>3</sub>	Nb <sub>2</sub> X	Nb <sub>2</sub> X	Nb <sub>3</sub> X	Nb <sub>5</sub> X
Al	-19	-29	-37	-40	-42	-44	-41	-40	-36	-28	-19
U	+2	+4	+5	+5	+5	+6	+6	+6	+5	+4	+3
Mo	-4	-6	-7	-8	-8	-9	-8	-8	-7	-5	-4

Tab. 2. Values in kJ (mole of atoms)<sup>-1</sup> for the predicted enthalpy of formation ( $\Delta h^{\text{for}}$ ) of binary niobium compounds [24].

	TiX <sub>5</sub>	TiX <sub>3</sub>	TiX <sub>2</sub>	Ti <sub>3</sub> X <sub>5</sub>	Ti <sub>2</sub> X <sub>3</sub>	TiX	Ti <sub>3</sub> X <sub>2</sub>	Ti <sub>5</sub> X <sub>3</sub>	Ti <sub>2</sub> X	Ti <sub>3</sub> X	Ti <sub>5</sub> X
Al	-26	-39	-50	-55	-57	-61	-57	-55	-50	-39	-26
U	0	0	0	0	0	0	0	0	0	0	0
Mo	-2	-4	-5	-5	-5	-5	-5	-5	-4	-3	-2

Tab. 3. Values in kJ (mole of atoms)<sup>-1</sup> for the predicted enthalpy of formation ( $\Delta h^{\text{for}}$ ) of binary titanium compounds [24].

## 5. Results

Five samples (details shown in Table 1) have been irradiated with the dpa  $\sim$  550-700 [36]. SRIM calculations [37] are performed under the conditions of iodine ion with 80 MeV and in the mode of *Detailed Calculation with Full Damages Cascades* with 500 ions. Post irradiation examinations are carried out by SEM and EDX. In SEM backscattered electron mode is applied to distinguish different chemical compositions.

### 5. 2. 1. Sample: UMo/Al

An UMo/Al sample without diffusion barrier is taken as a reference to show the generation of an irradiation induced interdiffusion layer. SRIM calculation shows the ion range is 5.32  $\mu\text{m}$  from the surface (Fig. 2). The displacement in the target distribution indicates the most damaged area is located at the UMo/Al interface. Averaging over the damage profile around 500 dpa are accumulated in the UMo layer.

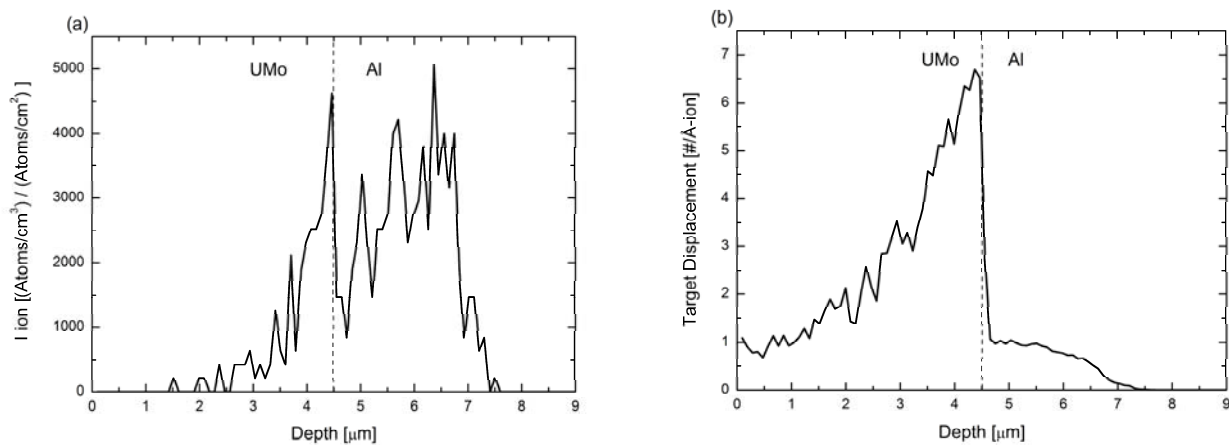


Fig. 2. SRIM simulation on (a) ion range and (b) total displacements in target of UMo/Al.

Its characterization by SEM and EDX is shown in Fig. 3. At the irradiated area a grey layer is generated (Fig. 3b) which is absent at the non-irradiated area (Fig. 3a). EDX indicates the existence of U, Mo and Al. This thin layer is an interaction layer between U-Mo alloy and Al formed during irradiation. EDX line scans also indicate the atom migration from Al to U after irradiation. Compounds like  $\text{UAl}_3$  and  $\text{UO}_2$  are formed in the interaction layer during irradiation [37].

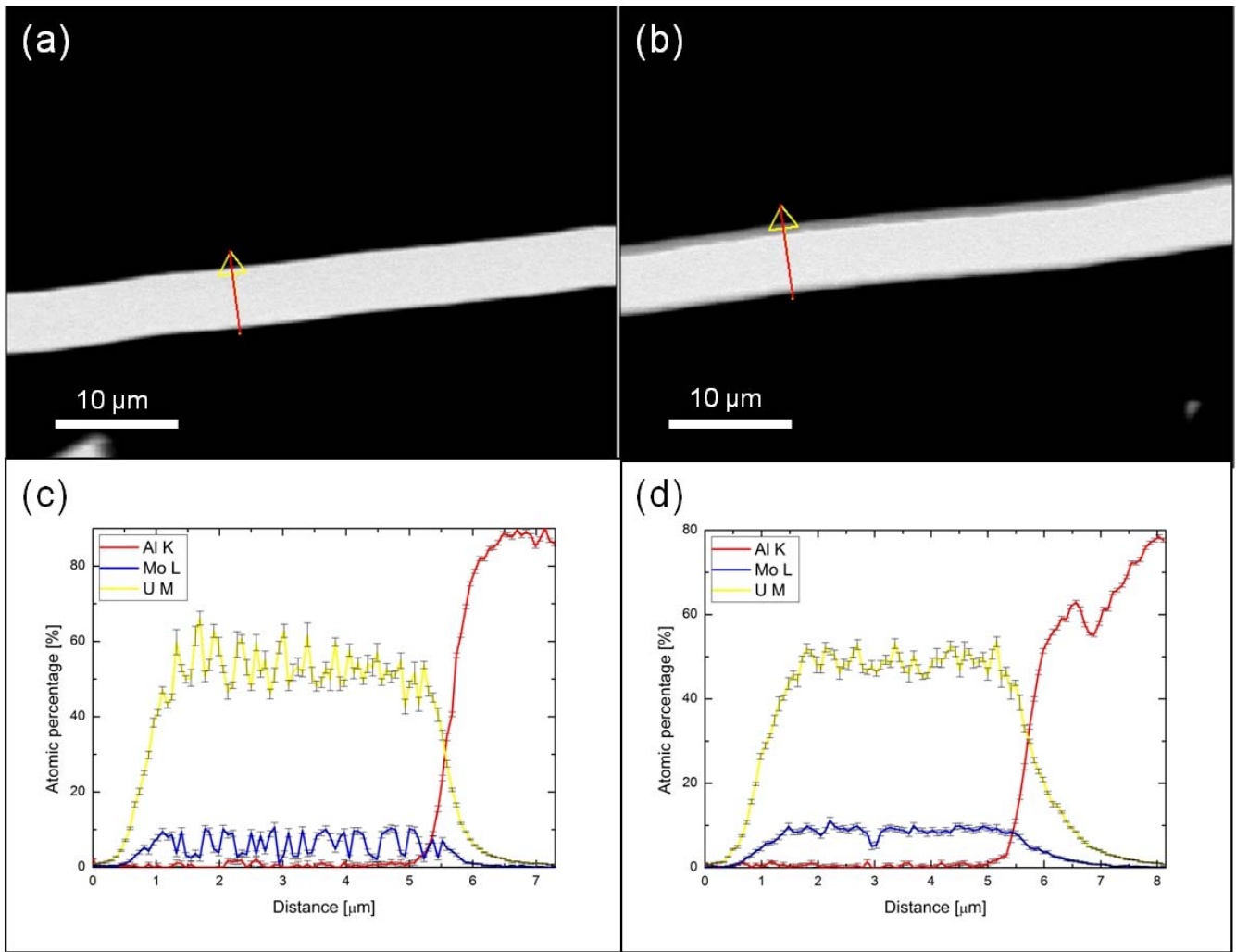


Fig. 3. SEM images and EDX line scans of UMo/Al. (a) SEM image taken at the non-irradiated area of the sample shows a sharp bright line as U-Mo layer in contact with Al matrix. (b) SEM image reveals the existence of an interaction layer with gray color at the interface between U-Mo and Al. (c) and (d) are EDX line scans of (a) and (b), respectively.

### 5. 2. 2. Sample: UMo/Nb/Al 1

UMo/Nb/Al 1 consists of a U-Mo layer with thickness 3.3 μm U-Mo and a 1.5 μm Nb coating. The iodine ion range is 5.75 μm from the surface and the most damaged areas are located at the interfaces especially at the Nb/Al interface (Fig. 4b).

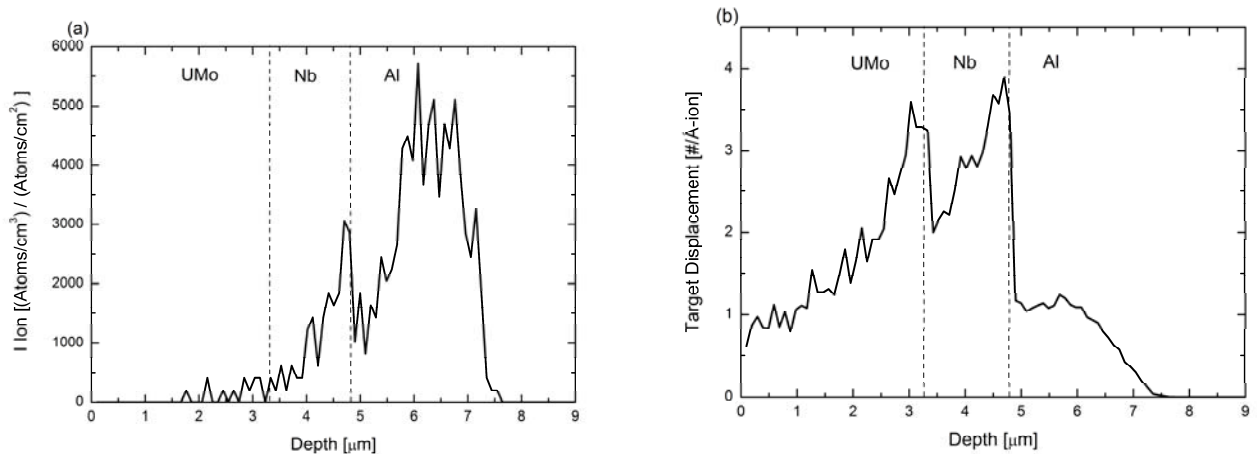


Fig. 4. SRIM simulation on (a) ion range and (b) total displacements in target of UMo/Nb/Al 1.

Post-irradiation examination by SEM (Fig. 5) shows an oxidation layer at the irradiated region due to the high temperature and iodine ion implantation at a depth of 5.8  $\mu\text{m}$  from the surface which coincides with the peak of ion range simulation by SRIM. No interaction layer is observed. However, EDX line-scans reveal the migration tendency of U and Al atoms after irradiation. The concentration curves of U and Al approach each other after irradiation. This phenomenon is in agreement with the ion recoil distribution by SRIM. It shows that after irradiation intermixing occurs.

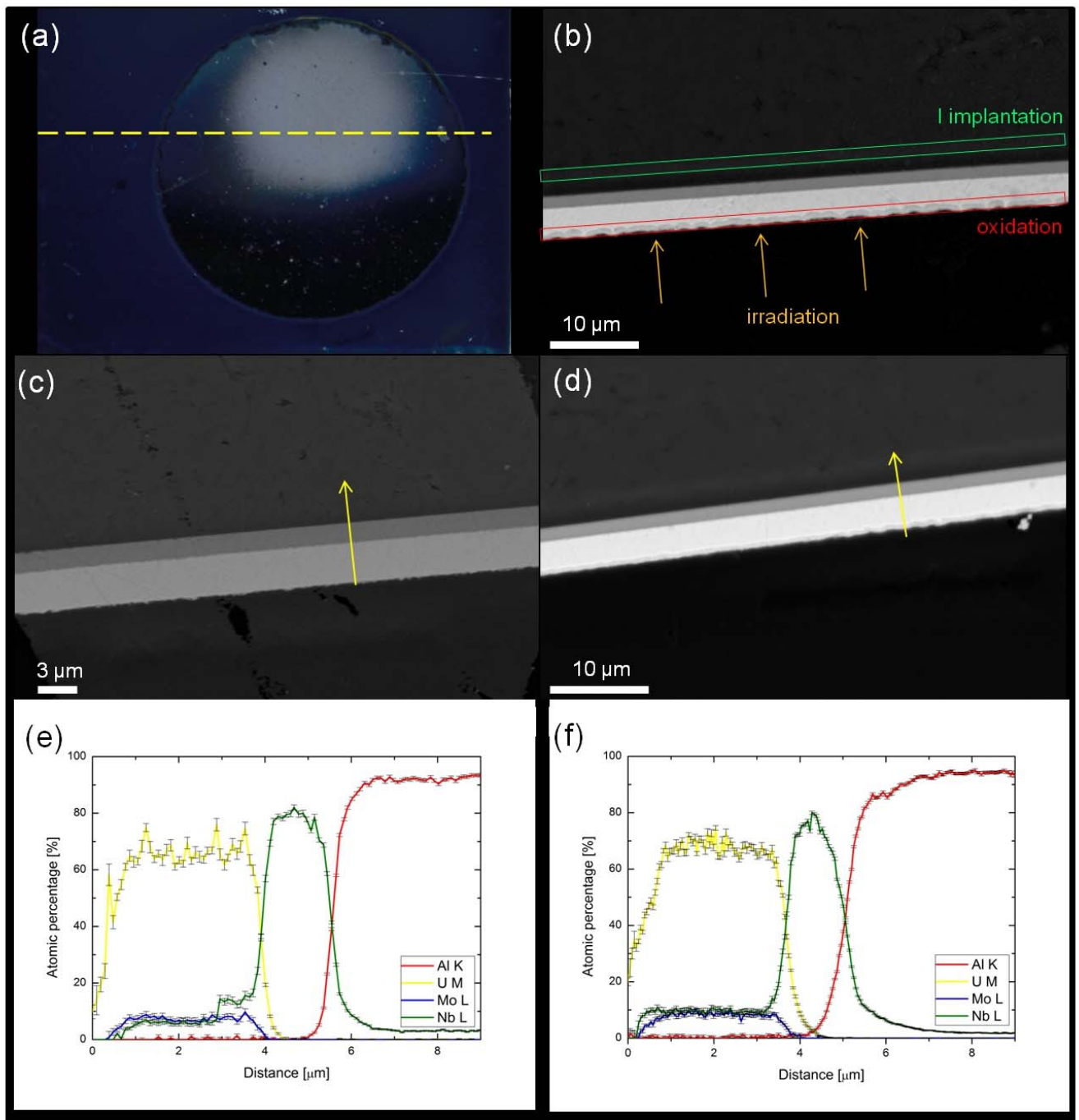


Fig. 5. (a) Optical image after irradiation shows the contour of beam spot. Within the region of beam spot, oxidation is observed and the dashed line indicates the cut for cross section preparation. (b) The irradiation direction, the oxidation layer, and Iodine implantation layer of UMo/Nb/Al 1 after irradiation. SEM images (c) and (d) are taken at non-irradiated and irradiated region, respectively. EDX line scans (e) and (f) correspond to (c) and (d), respectively.

### 5. 2. 3. Sample: UMo/Nb/Al 2

UMo/Nb/Al 2 has a thinner U-Mo layer of 2.2  $\mu\text{m}$  and a 1.5  $\mu\text{m}$  Nb layer like UMo/Nb/Al 1. The ion range is 7.23  $\mu\text{m}$  (Fig. 6a). Target displacement distribution indicates at the Nb/Al interface the number of displacement is highest (Fig. 6b).

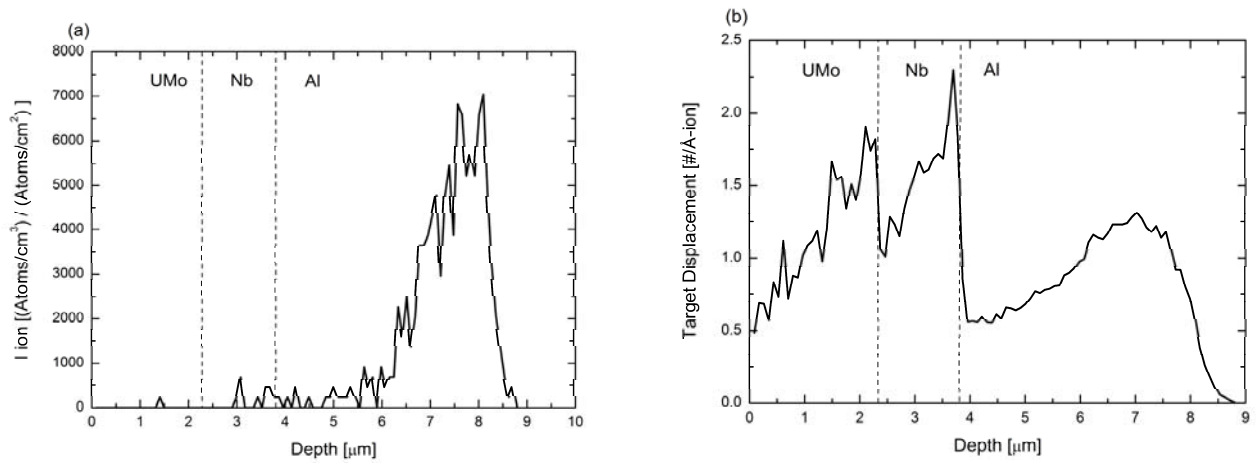


Fig. 6. SRIM simulation on (a) ion range and (b) total displacements in target of UMo/Nb/Al 2.

SEM also shows an oxidation layer and iodine implantations in Fig. 3a and 3c but no existence of an interaction layer. EDX line scans are shown in Fig. 4. The tendency of ion migration is observed. One can clearly distinguish the differences between Nb peak at non-irradiated and at irradiated area. EDX line scans at the boundary of irradiated region are made parallel to the interfaces (Fig. 7d, Fig. 8c and 8d). It is observed that the compositions vary along the interfaces. The variations of U and Nb along the interface shown in Fig. 5c are very smooth and the line scans reveal the intermixing of U and Nb atoms. Along the interface of Nb and Al a pronounced composition variation is observed. After irradiation Al atoms migrate toward the Nb layer.

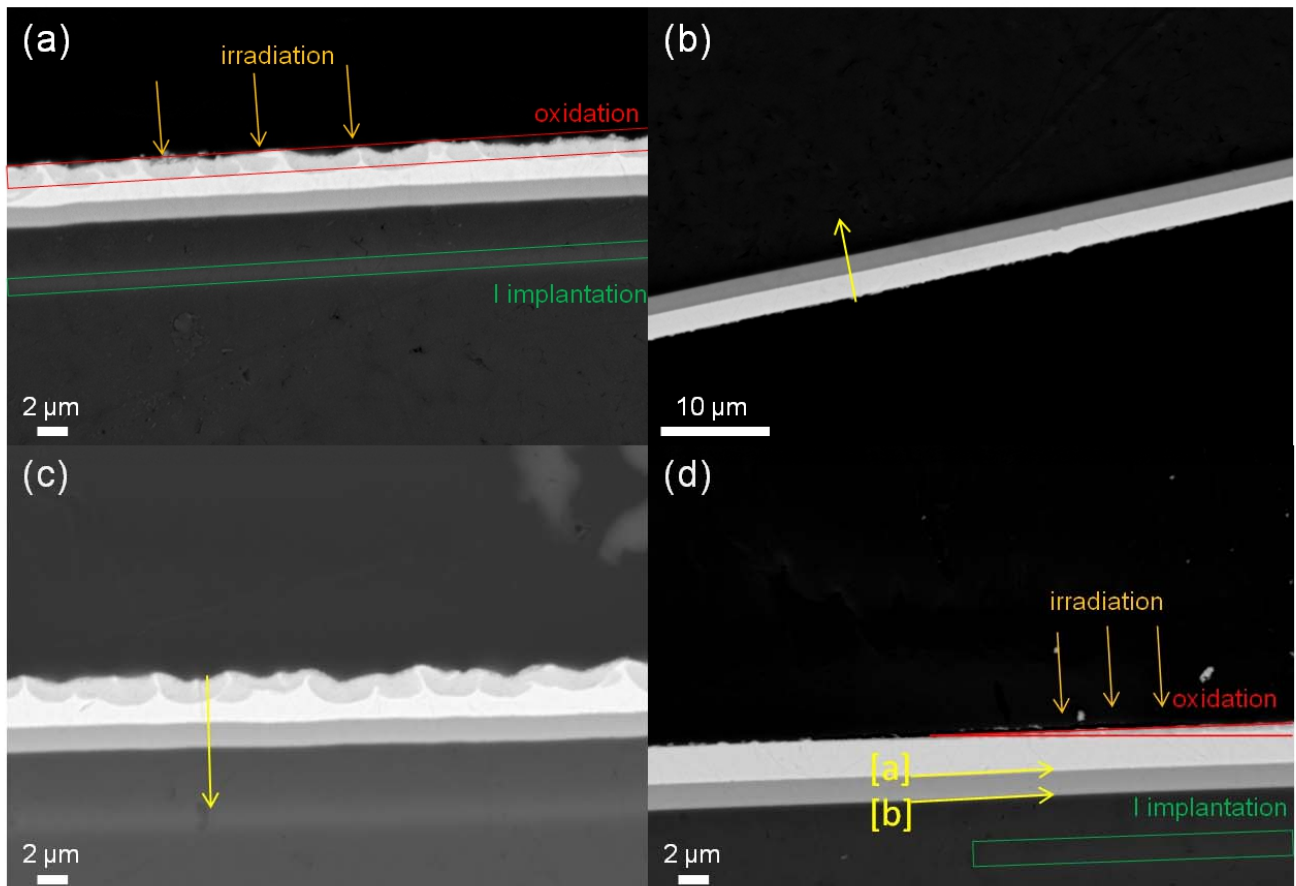


Fig. 7. SEM images of UMo/Nb/Al 2: (a) the direction of ion irradiation, the oxidation layer and the iodine implantation layer at the irradiated region are shown (b) The arrow shows the direction of EDX line scan at non-irradiated region perpendicular to the layers. (c) The arrow shows the direction of EDX line scan at irradiated region perpendicular to the layers and (d) the arrow [a] and [b] show the direction of EDX line scans at the boundary between non-irradiated and irradiated region parallel to the (U-Mo)/Nb and the Nb/Al interfaces, respectively.

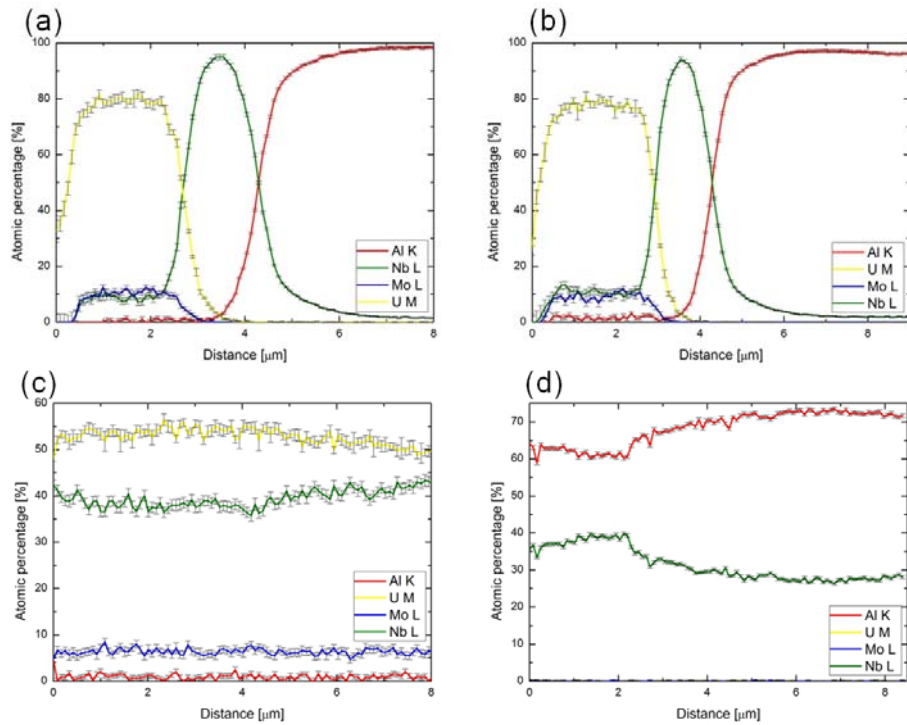


Fig. 8. EDX line scans of UMo/Nb/Al 2: (a) and (b) are made through the layers perpendicularly correspond to Fig. 7. (b) and (c), respectively. (c) and (d) are made through the directions parallel to the (U-Mo)/Nb and the Nb/Al interface correspond to Fig. 7. (d)[a] and [b], respectively.

#### 5. 2. 4. Sample: UMo/TiN/Al 1

UMo/TiN/Al 1 consists of a U-Mo layer with thickness 3.3  $\mu\text{m}$  and a TiN layer with thickness of 450 nm. The iodine ion range is 5.45  $\mu\text{m}$  from the surface. Most damage occurs at the UMo/TiN interface and little displacements happens at TiN layer (Fig. 9).

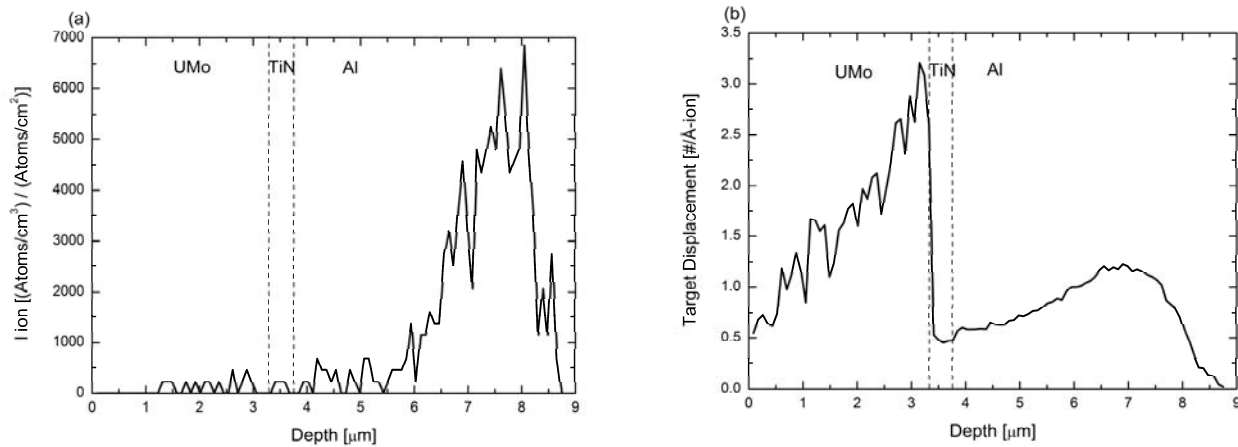


Fig. 9. SRIM simulation on (a) ion range and (b) total displacements in target of UMo/TiN/Al 1.

SEM images (Fig. 10) show the same behavior as the samples with Nb as diffusion barrier, iodine implantation, subsequent oxidation but no interaction layer at the irradiated area. Within the resolution limit of 1  $\mu\text{m}$  EDX line scans along the interface near the boundary exhibit no tendency of atom migration either at the (U-Mo)/TiN interface nor at TiN/Al (Fig. 10c and 10d).

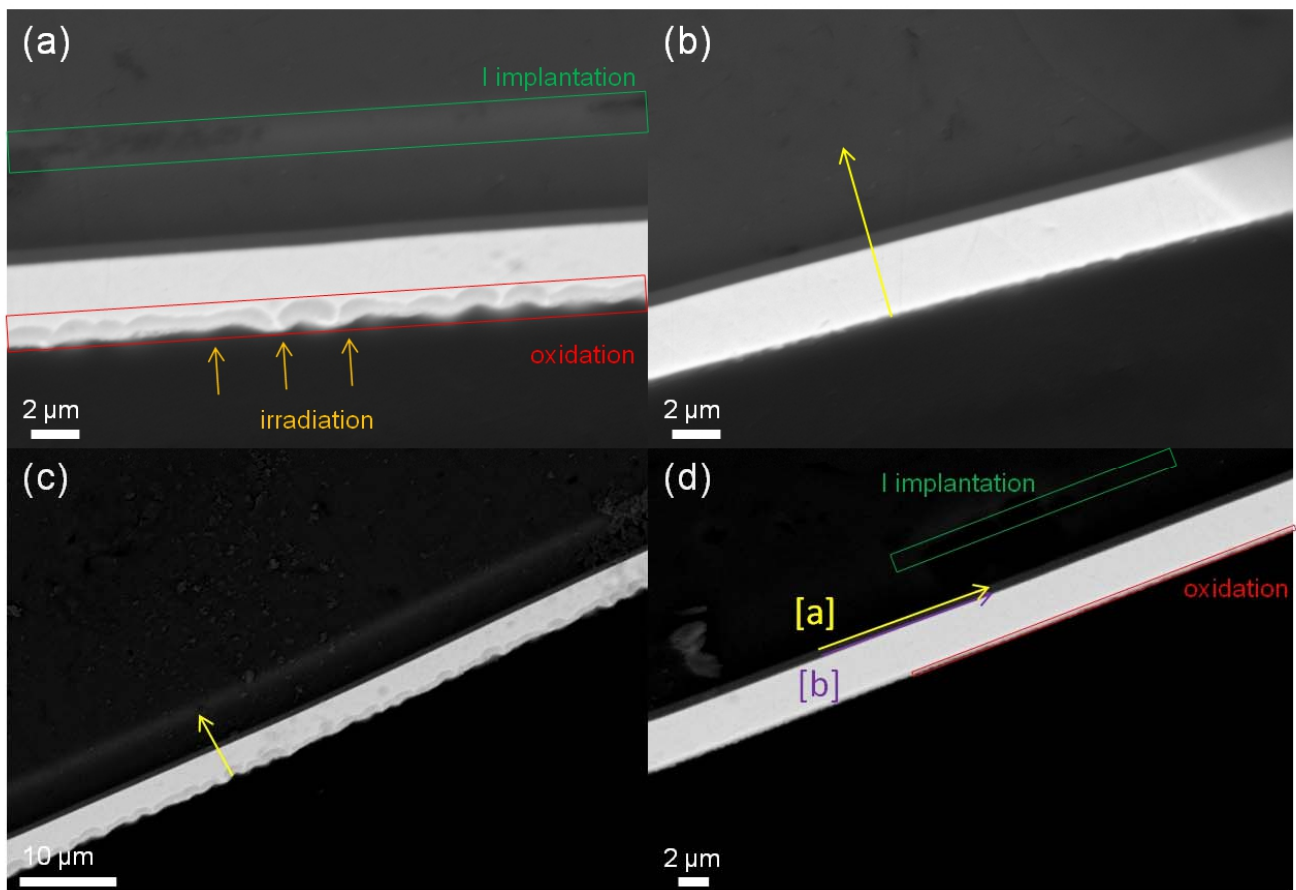


Fig. 10. SEM images of UMo/TiN/Al 1: (a) the direction of ion irradiation, the oxidation layer and the iodine implantation layer at the irradiated region are indicated (b) the arrow shows the direction of EDX line scan at non-irradiated region perpendicular to the layers and (c) the arrow shows the direction of EDX line scan at irradiated region perpendicular to the layers and (d) the arrow [a] and [b] show the direction of EDX line scans at the boundary between non-irradiated and irradiated region parallel to the Al/TiN and the TiN/ (U-Mo) interfaces, respectively.

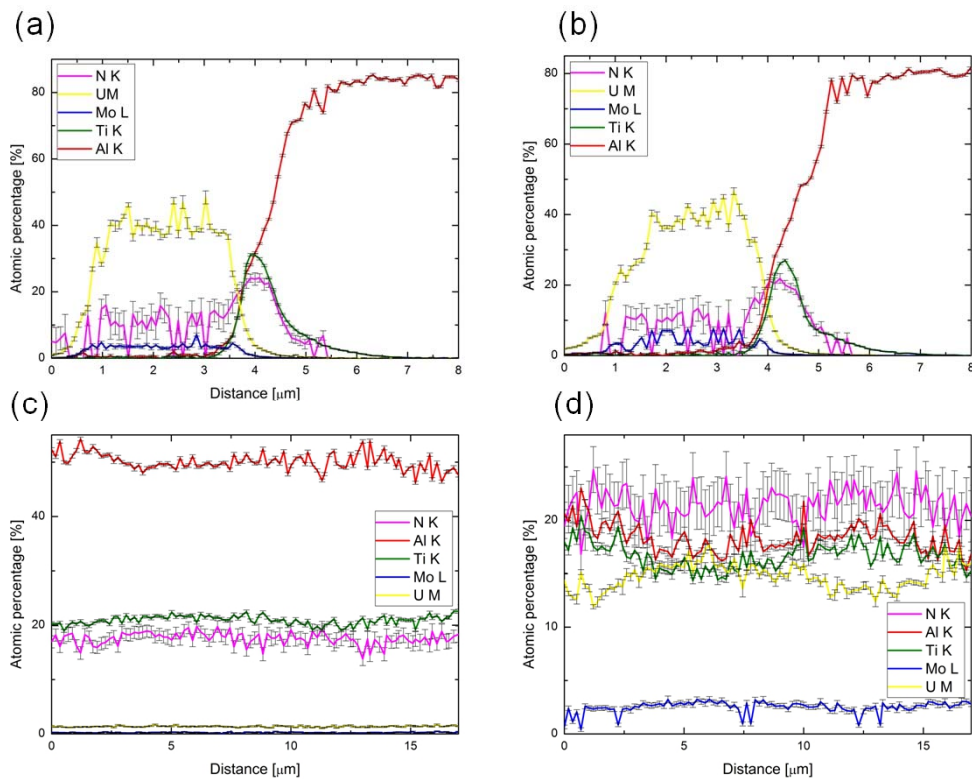


Fig. 11. EDX line scans of UMo/TiN/Al 1: (a) and (b) are made through the layers perpendicularly correspond to Fig. 10. (b) and (c), respectively. (c) and (d) are made through the directions parallel to the the Al/TiN and the TiN/(U-Mo) interface correspond to Fig. 10. (d)[a] and [b], respectively.

### 5. 2. 5. Sample: UMo/TiN/Al 2

UMo/TiN/Al 2 has a U-Mo layer with thickness of 3.3  $\mu\text{m}$  and a 230 nm thin TiN layer. The ion range is 6.84  $\mu\text{m}$  and target displacement indicates most displacements occur in the UMo layer (Fig. 12).

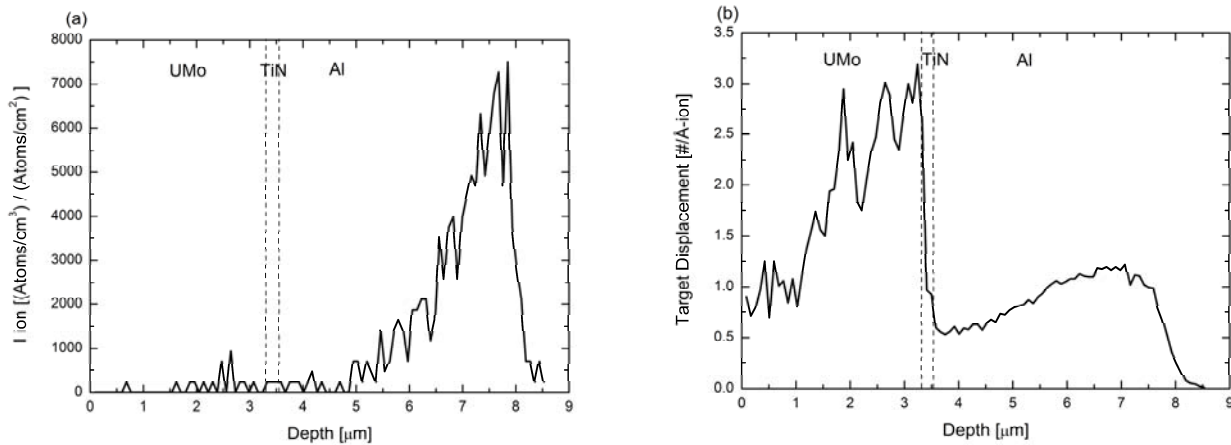


Fig. 12. SRIM simulation of (a) ion range and (b) total displacements in target of UMo/TiN/Al 2.

SEM examinations show no interaction neither on the (U-Mo)/TiN interface nor on the TiN/Al interface. EDX examinations (Fig. 14) perpendicular to the layers exhibit the same composition at non-irradiated and irradiated area. Fig. 13d indicates the directions of EDX line scans at the boundary along the layer interface. With EDX line scans shown in Fig. 14c, it is observed that at the interface between U-Mo and Ti layer the composition of U increases and the composition of Ti decrease. On the other hand, it is observed that the compositions of Ti and Al stay the same at the boundary of non-irradiated and irradiated region.

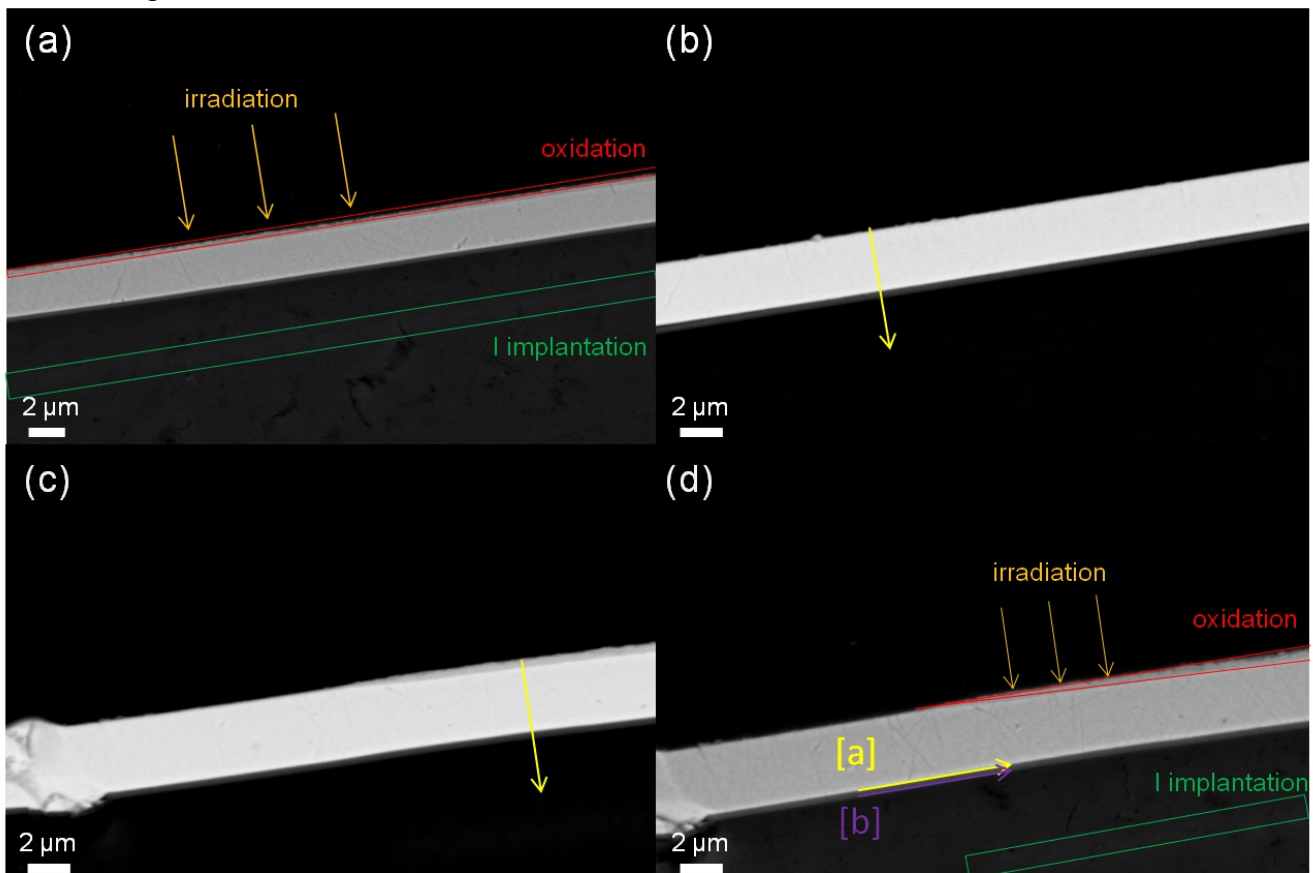


Fig. 13. SEM images of UMo/TiN/Al 2: (a) the direction of ion irradiation, the oxidation layer and the Iodine implantation layer at the irradiated region are indicated (b) The arrow shows the direction of EDX line scan at non-irradiated region perpendicular to the layers (c) the arrow shows the direction of EDX line scan at irradiated region perpendicular to the layers and (d) the arrow [a] and [b] show the direction of EDX line scans at the boundary between non-irradiated and irradiated region parallel to the (U-Mo)/TiN and the TiN/Al interfaces, respectively.

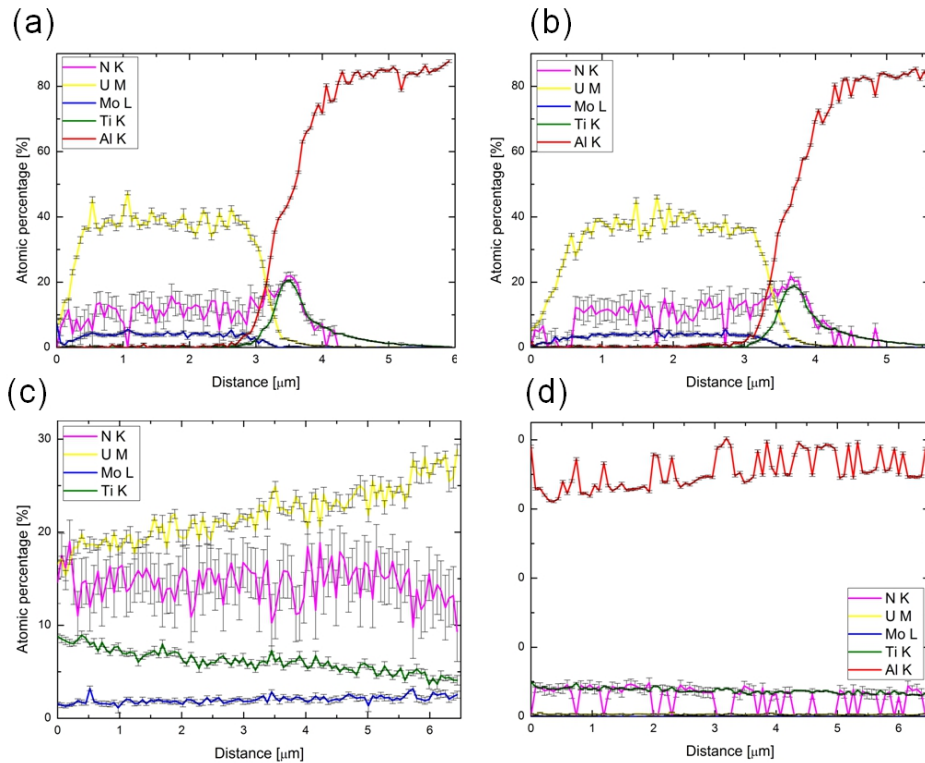


Fig. 14. EDX line scans of UMo/TiN/Al 1: (a) and (b) are made through the layers perpendicularly in correspond to Fig. 13. (b) and (c), respectively. (c) and (d) are made through the directions parallel to the (U-Mo)/TiN and the TiN/Al interface in correspond to Fig. 13. (d)[a] and [b], respectively

## 6. Discussion

SEM characterization shows no interaction layer in both Nb and TiN sandwich structures. However, EDX examination indicates the migration tendency of atoms after irradiation. In UMo/Al the generation of an interaction layer after irradiation coincides with the atom migration observed by EDX line scans. This combination of atom mixing and the formation of an IDL does not apply in coated samples. No IDL is found in the coated samples by SEM but EDX indicates the mixing tendency of atoms. This can be considered as ion beam mixing induced solid solution and is usually explained by *diffusion in local thermal-spikes* [39] and *mixing in global thermal-spikes* [40-41].

Nb as a diffusion barrier shows no interaction layer but ion beam mixing effect induced solid solution. The ion beam mixing effect is proportional to the ion penetration depth. The variation of the composition changes rather prominently in UMo/Nb/Al 2 case. It is reported that a thin Nb<sub>3</sub>Al layer can be formed at the Nb/Al interface under He ion irradiation [25]. However, in our case SEM measurement shows no generation of this extra layer. This difference might result from the characterization methods (SEM and XTEM) and irradiation conditions (ion species and energy). Atomic migration is observed which is in agreement with SRIM simulation: Nb atoms migrate toward U and Al atoms move toward Nb.

TiN as a diffusion barrier isolates all interactions among the sandwich samples. With a 450 nm TiN layer, UMo/TiN/Al 1, atomic mixing effect cannot be observed at the interfaces. In UMo/TiN/Al 2 with a 230 nm TiN, atomic mixing effect is observed at the UMo/TiN interface but not at the TiN/Al interface. It reveals that as a diffusion barrier TiN is very adequate and promising.

## 7. Conclusions

Based on metallurgical and chemical considerations, Nb and TiN have been selected as the diffusion barriers. Indeed after irradiation a complete suppression of the IDL is observed. Already a 230 nm thin layer of TiN isolates all interaction between U and Al.

## 8. Acknowledgements

The authors want to express our sincere thanks to Rainer Emiling from Fakultät für Elektro- und Informationstechnik, Technische Universität München for the assistance of TiN thin film fabrications. Also we would like to convey our gratitude to the beamline scientists W. Carli et al in Maier-Leibnitz-Laboratorium for all the instructions and assistances during the beam time. This work is supported by a combined grant (FRM 0911) from Bundesministerium für Bildung und Forschung (BMBF) and the Bayerisches Staatsministerium für Wissenschaft, Forschung und Kunst (StMWFK).

## 9. References

- [1] N. Wieschalla, A. Bergmaier, P. Boeni, K. Boening, G. Dollinger, R. Grossman, W. Petry, A. Roehrmoser and J. Schneider, Heavy ion irradiated of U-Mo/Al dispersion fuel, *J. Nucl. Mater.*, 2006, 357 (1-3), p 191-197
- [2] A. Roehrmoser, Untersuchungen zur Kuehlbarkeit eines neuartigen Kompaktkerns fuer Forschungsreaktoren, Diplomarbeit, Technische Universit□at Muenchen, 1984.
- [3] S. van den Berghe et al., Transmission electron microscopy investigation of irradiated U7wt%Mo dispersion fuel. *Journal of Nuclear Materials*, 2008, 375, p 340-346
- [4] K. Colon and D. Sears, Neutron powder diffraction of UMo fuel irradiated to 60% burn-up, *Research Reactor Fuel Management (RRFM)*, Lyons, 2007.
- [5] S.L. Hayes et al., Modelling RERTR experimental fuel plates using the palte code, *Reduced Enrichment for Research and Test Reactors (RERTR)*, Chicago, 2002
- [6] J.M. Park et al., Phase stability and diffusion characteristics of U-Mo-X (X=Si, Al, Zr or Ti) alloys, *Reduced Enrichment for Research and Test Reactors (RERTR)*, Boston, 2005
- [7] C.D. Cagle and L.B. Emler, Slug ruptures in the Oak Ridge National Laboratory pile, *Technical Report ORNL-170*, Oak Ridge National Laboratory, 1948
- [8] G.L. Hofman et al., Post irradiation analysis of low enriched U-Mo/Al dispersion fuel miniplate tests, *RERTR 4&5*, *Reduced Enrichment for Research and Test Reactors (RERTR)*, 2004
- [9] P. Lemoine et al., UMo dispersion fuel results and status of qualification programs, *Research Reactor Fuel Management (RRFM)*, Munich, 2004
- [10] A. Leenaers, S. Van den Berghe, E. Koonen, C. Jarousse, F. Huet, M. Troabas, M. Boyard, S. Guillot, L. Sannen, and M. Verwert, Post-Irradiation Examination of Uranium-7 wt.% Molybdenum Atomized Dispersion Fuel, *J. Nucl. Mater.*, 2004, 335(1), p 39-47
- [11] R.O. Williams, Terminal report on ORNL slug problem - causes and prevention, *Technical Report CF-50-7-160*, Oak Ridge National Laboratory, 1950
- [12] L.S. DeLuca et al., Rate of growth of diffusion layers in U-Al and U-AlSi couples, *Technical Report KAPL-1747*, Knolls Atomic Power Laboratory, 1957
- [13] G. Hofman et al., Results of Low-Enriched U-Mo Miniplates from RERTR-6 and -7A Irradiation, *Reduced Enrichment for Research and Test Reactors (RERTR)*, Cape Town, 2006
- [14] M. Cornen et al., Physico-chemical aspects of modified UMo/Al interaction, *Research Reactor Fuel Management (RRFM)*, Lyons, 2007
- [15] M.P. Johnson and W.A. Holland, Irradiation of U-Mo base alloys, *Technical Report NAA-SR-6262*, *Atomics International*, 1964
- [16] W.C. Thurber and R.J. Beaver, Development of Silicon modified 48wt%U-Al alloys for aluminum plate type fuel elements, *Technical Report ORNL-2602*, Oak Ridge National Laboratory, 1959

- [17] R.J. Van Thyne et al., Transformation kinetics of Uranium-Niobium and ternary Uranium-Molybdenum base alloys, Transactions American Society for Metals, 49, p 576-597, 1957
- [18] M. Rodier et al., Effects of Ti in the UMo/Al system: preliminary results, Research Reactor Fuel Management (RRFM), Lyons, 2007
- [19] A. Izhutov et al., The status of LEU U-Mo fuel investigation in the MIR reactor, Reduced Enrichment for Research and Test Reactors (RERTR), Beijing, 2009
- [20] G.A. Birzhevoy et al., Results of post-irradiation examination of the (U-Mo)-Aluminum matrix interaction rate, Research Reactor Fuel Management (RRFM), Lyons, 2007
- [21] H.A. Saller, Uranium alloy newsletter No.13. Technical Report WASH-295, Battelle Memorial Institute, 1955
- [22] D.D. Keiser et al., Characterization and testing of monolithic RERTR fuel plates, Research Reactor Fuel Management (RRFM), Lyons, 2007
- [23] T. B. Massalski, H. Okamoto, P.R. Subramanian, L. Kacprzak, Binary Alloy Phase Diagrams, The Mater. Inform. Soci., 1990
- [24] F. R. de Boer, R. Boom, W.C. M. Mattens, A. R. Miedema and A. K. Niessen, Cohesion in Metals: Transition in Metal Alloys, North-Holland, 1988
- [25] N. Li, M.S. Martin, O. Anderoglu, A. Misra, L. Shao, H. Wang, and X. Zang, He Ion Irradiation Damage in Al/Nb Multilayers, J. App. Phys. 2009, 105, 123522
- [26] A.L. Izhutov, V.V. Alexandrov, A.E. Novoselov, V.A. Starkov, V.E. Fedoseev, V.V. Pimenov, A.V. Sheldyakov, V. Yu. Shishin, V.V. Yakovlev, I.V. Dobrikova, A.V. Vatulin, V.B. Suprun, and G.V. Kulakov, The Main Results Of Investigation Of Modified Dispersion LEU U-Mo Fuel Tested In The MIR Reactor, RERTR 2010
- [27] R. Jungwirth, H. Breikreutz, W. Petry, A. Röhrmoser, W. Schmid, H. Palancher, C. Bertrand-Drira, C. Sabathier, X. Iltis, N. Tarisien, and C. Jarousse, Optimization of the Si Content in UMo-Al(Si) Fuel Plates, RERTR 2009
- [28] MCNP Library, <http://atom.kaeri.re.kr>
- [29] C.K. Gupta, Materials In Nuclear Energy Applications, CRC Press Inc., 1989
- [30] D. Emendoerfer, K.H. Hoecker, Theorie der Kernreaktoren, Wissenschaftsverlag Berlin, 1982
- [31] W. Schmid, S. Dirndorfer, R. Grossmann, H. Juranowitsch, W. Petry and C. Jarousse, Research Reactor Fuel Management (RRFM), 2010
- [32] L. Gao, J. Gstöttner, R. Emling, C. Linsmeier, M. Balden, A. Wiltner, W. Hansch, D. Schmitt-Landsiedel, Microelectron. Eng., 2005, 82: 3–4. p 296-300
- [33] R. Jungwirth, T. Zweifel, H.-Y. Chiang, W. Petry, S. Van den Berghe and A. Leenaers, Heavy ion irradiation of UMo/Al samples with protective Si and ZrN layers (SELENIUM), Research Reactor Fuel Management (RRFM), 2011
- [34] S. Matteson and M-A. Nicolet, Metalstable Materials Formation by Ion Implantation, eds., by S.T. Picraux and W.J. Choyke, (North-Holland, Amsterdam, 1982) p3
- [35] A. Madan, I.W. Kim, S.C. Cheng, P. Yashar, V.P. Dravid, S.A. Barnett, Mutual promotion effect of crystal growth in TiN/SiC nanomultilayers, Phys. Rev. Lett. 78 (1997) 1743
- [36] R. M. Hengstler-Eger et al., Heavy ion irradiation induced dislocation loops in AREVA's M5<sup>®</sup>, J. Nucl. Mater., to be published.
- [37] J. F. Ziegler, J. P. Biersack, and U. Littmark, The Stopping And Range of Ion in Solids, Pergamon Press, New York, 1985
- [38] H. Palancher, N. Wieschalla, P. Martin, R. Tucoulou, C. Sabathier, W. Petry, J.-F. Berar, C. Valot, and S. Dubois, Uranium–Molybdenum Nuclear Fuel Plates Behaviour Under Heavy Ion Irradiation: An X-Ray Diffraction Analysis, J. Nucl. Mater., 2006, 385, p 449-455
- [39] P. Borgesen, D. A. Lilienfeld, H. H. Johnson, Appl. Phys. Lett. 57 (1990) p1407
- [40] W. Bolse, Mat. Sci. Eng. R12 (1994) p 53
- [41] W. Bolse, Nucl. Inst. Meth. B80/81 (1993) p 137